Superfluid shells for trapped fermions with mass and population imbalance

G.-D. Lin, W. Yi and L.-M. Duan
FOCUS center and MCTP, Department of Physics, University of Michigan, Ann Arbor, MI 48109

We map out the phase diagram of strongly interacting fermions in a potential trap with mass and population imbalance between the two spin components. As a unique feature distinctively different from the equal-mass case, we show that the superfluid here forms a shell structure which is not simply connected in space. Different types of normal states occupy the trap regions inside and outside this superfluid shell. We calculate the atomic density profiles, which provide an experimental signature for the superfluid shell structure.

PACS numbers:

The recent experimental advance on superfluidity in polarized ultracold Fermi gas has raised strong interest in studying the phase configuration of this system [1, 2, 3, 4, 5, 6, 7, 8, 9, 10, 11]. The experiments have suggested a phase separation picture with a superfluid core surrounded by a shell of normal gas [1, 2, 3, 4]. This picture has been confirmed also by a number of theoretical calculations of the atomic density profiles in the trap [8, 9, 10, 11]. As Feshbach resonances between different atomic species with unequal mass have been reported [12], the next step is to consider the properties of strongly interacting Fermi gas with both mass and population imbalance between the two spin components. There have been a few recent theoretical works in this direction [13, 14], with focus on the properties of a homogeneous gas.

In this work, we consider the properties of a *trapped* strongly interacting Fermi gas with mass and population imbalance. We map out its zero temperature phase diagram in a harmonic trap (generally anisotropic) as a function of few universal parameters. Compared with the equal-mass case, the two-specie Fermi mixture (^{6}Li-^{40}K mixture for instance) shows a very different picture of phase separation: it supports a superfluid shell state in the intermediate trap region, with normal gases of different characters filling the center and the edge of the trap. This unusual phase separation picture with non-monotonic superfluid order parameter in space only occurs for trapped fermions with unequal mass. We provide an intuitive explanation for the phenomenon, and show how to detect it by measuring the atomic density profiles. This superfluid shell state is not simply connected in space, so it may support interesting vortex structure under rotation of the trap.

Strongly interacting Fermi gas near a wide Feshbach resonance can be well described by the following single-channel Hamiltonian:

$$\begin{aligned} H &= \sum_{\mathbf{k},\sigma} \left(\epsilon_{\mathbf{k}\sigma} - \mu_\sigma\right) a^\dagger_{\mathbf{k},\sigma} a_{\mathbf{k},\sigma} \\ &+ \left(U/\mathcal{V}\right) \sum_{\mathbf{q},\mathbf{k},\mathbf{k}'} a^\dagger_{\mathbf{q}/2+\mathbf{k},\uparrow} a^\dagger_{\mathbf{q}/2-\mathbf{k},\downarrow} a_{\mathbf{q}/2-\mathbf{k}',\downarrow} a_{\mathbf{q}/2+\mathbf{k}',\uparrow} \end{aligned} \quad (1)$$

where $\epsilon_{\mathbf{k}\sigma} = \mathbf{k}^2/(2m_\sigma)$ with m_σ denoting the mass of species-σ (or called spin σ, with $\sigma = \uparrow, \downarrow$ and $\hbar = 1$), $\mathcal{V}$ is the quantization volume, and $a^\dagger_{\mathbf{k},\sigma}$ is the fermionic creation operator for the $\mathbf{k}\sigma$ mode. The bare atom-atom interaction rate U is connected with the physical scattering length a_s through the renormalization relation $1/U = 1/U_p - (1/\mathcal{V})\sum_{\mathbf{k}} 1/(2\epsilon_{\mathbf{k}})$ with $U_p = 4\pi a_s/(2m_r)$ ($m_r = m_\uparrow m_\downarrow/(m_\uparrow + m_\downarrow)$ is the reduced mass). We take the local density approximation so that $\mu_\uparrow = \mu_{\mathbf{r}} + h$, $\mu_\downarrow = \mu_{\mathbf{r}} - h$, $\mu_{\mathbf{r}} = \mu - V(\mathbf{r})$, where $V(\mathbf{r}) = \sum_{i=x,y,z} \beta_i \mathbf{r}_i^2/2$ is the harmonic trapping potential, which, without loss of generality, has been assumed to be the same for the two components. The chemical potential μ at the trap center and the chemical potential imbalance h are determined from the total atom number $N = N_\uparrow + N_\downarrow$ and the population imbalance $p = (N_\uparrow - N_\downarrow)/N$ through the number equations below.

Our calculation method is based on a simple extension of the formalism described in Ref. [8] to the unequal mass case. Under the mean-field approximation, the thermodynamical potential $\Omega = -T\ln[\mathrm{tr}(e^{-H/T})]$ (T is temperature) can be written as [16]

$$\begin{aligned} \Omega &= -\mathcal{V}|\Delta|^2/U + \sum_{\mathbf{k}} \left[\epsilon_{\mathbf{k}\downarrow} - \mu_\downarrow - E_{\mathbf{k}\downarrow}\right] \\ &\quad -T\sum_{\mathbf{k}} \ln\left[\left(1 + e^{-E_{\mathbf{k}\uparrow}/T}\right)\left(1 + e^{-E_{\mathbf{k}\downarrow}/T}\right)\right] \end{aligned} \quad (2)$$

where $E_{\mathbf{k}\uparrow,\downarrow} = E_{\mathbf{k}} \mp (h + \alpha\epsilon_{\mathbf{k}r})$ with $E_{\mathbf{k}} \equiv \sqrt{(\epsilon_{\mathbf{k}r} - \mu_{\mathbf{r}})^2 + \Delta^2}$, $\epsilon_{\mathbf{k}r} \equiv \mathbf{k}^2/(4m_r)$, and $\alpha \equiv (m_\uparrow - m_\downarrow)/(m_\uparrow + m_\downarrow)$. If one of the energies $E_{\pm,\mathbf{k}}$ has one or two zero(s) in $\mathbf{k}$-space, it signals the presence of the type-I or type-II breached-pair (Sarma) states [5, 7, 8, 15] (called the BP1 or BP2 states, respectively). The BP states represent a spatially homogeneous superfluid, but they differ from the conventional BCS states by a phase separation in the momentum space and by a topological change of the Fermi surface for the excess fermions. To determine the phase at different trap regions, we search for the global minimum of the thermo-potential Ω with respect to the variational parameter Δ instead of using the gap equation $\partial\Omega/\partial\Delta = 0$, as the latter may give unstable or metastable phases as remarked in Ref. [8].

The μ and h are determined from the two number equations $N_\sigma = \int d^3\mathbf{r} n_{\mathbf{r}\sigma}$ integrated over the trap. The local atomic density $n_{\mathbf{r}\sigma}$, derived from the thermodynamical potential Ω as $\partial\Omega/\partial\mu_\sigma = -n_{\mathbf{r}\sigma}\mathcal{V}$, has the expression

$$n_{\mathbf{r}\sigma} = \frac{1}{\mathcal{V}}\sum_{\mathbf{k}}[u^2_{\mathbf{k}} f(E_{\mathbf{k},\sigma}) + v^2_{\mathbf{k}} f(-E_{\mathbf{k},-\sigma})], \qquad (3)$$

where the parameters $u^2_{\mathbf{k}} = (E_{\mathbf{k}} + (\epsilon_{\mathbf{k}r} - \mu_{\mathbf{r}}))/(2E_{\mathbf{k}})$, $v^2_{\mathbf{k}} = (E_{\mathbf{k}} - (\epsilon_{\mathbf{k}r} - \mu_{\mathbf{r}}))/(2E_{\mathbf{k}})$, and the Fermi distribution $f(E) \equiv 1/\left(1 + e^{E/T}\right)$. For convenience, we take $- \uparrow = \downarrow$ and vice versa. The above mean-field formalism is also identical to the G_0G diagram scheme if we interpret Δ at finite temperature as the total gap which includes contributions from both the order parameter and the pseudogap associated with the pair fluctuations [8, 11].

We calculate the phase diagram of the trapped fermions in terms of several dimensionless universal parameters. For that purpose, the unit of energy is chosen to be the Fermi energy E_F at the center of the trap for N non-interacting fermions with an effective mass of $2m_r$ and with equal population for the two components. Under the local density approximation, one finds $E_F = (3N\sqrt{\beta_x\beta_y\beta_z})^{1/3}/\sqrt{2m_r}$ from this definition. The trapping potential $V(\mathbf{r})$ has the dimensionless form $V(\mathbf{r})/E_F = \sum_i \widetilde{r}_i^2$, where the normalized coordinates $\widetilde{r}_i \equiv r_i/R_i$ and $R_i \equiv \sqrt{2E_F/\beta_i}$ is the Thomas-Fermi radius along the ith direction. The momentum $\mathbf{k}$ and the temperature T are measured in the units of $k_F \equiv \sqrt{2(2m_r)E_F}$ and $T_F \equiv E_F/k_B$, respectively. The system properties then only depend on four dimensionless parameters k_Fa_s, T/T_F, the population imbalance p, and the mass mismatch α. In the following calculation, we take $\alpha = 0.74$ corresponding to the ^{40}K-^{6}Li mixture, as the latter is the most likely experimental system for the two-specie Fermi gas.

In Fig. 1, we map out the zero-temperature phase diagrams for trapped fermions as a function of the population imbalance p at several characteristic interaction strengths k_Fa_s. The system shows a rich picture of phase separation in the trap. First, on the BCS side of resonance with $(k_Fa_s)^{-1} = -1$ (Fig. 1(a)), even in the equal population case ($p = 0$), we cross four different phases from the trap center to the edge. The trap center is occupied by a normal mixture state with the heavy fermions (^{40}K) in excess (denoted as $\mathrm{NM_K}$), which is surrounded by a shell of BCS superfluid phase (denoted as SF). Further out, there is a shell of a normal mixture but now with the light fermions (^{6}Li) in excess (denoted as $\mathrm{NM_{Li}}$). The trap edge is occupied by the single component normal gas of light fermions (denote as $\mathrm{NP_{Li}}$). The system behavior becomes significantly more complicated compared with the equal mass case [8, 9, 10, 11], where instead of several phases, there is only one superfluid phase over the whole trap in the corresponding configuration. Note that under the local density approximation,

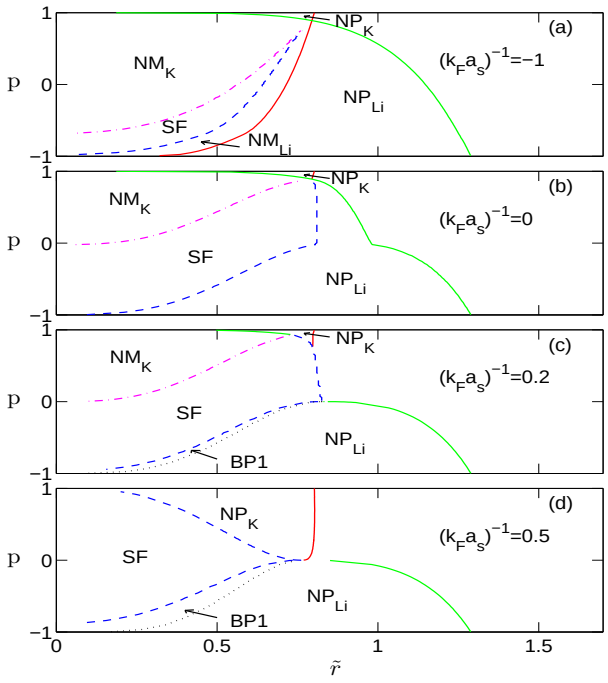

FIG. 1: (color online) The zero temperature phase diagrams for trapped ^{6}Li-^{40}K mixture near a Feshbach resonance. The phases include the BCS superfluid state (SF), the breached pair phase of type 1 (BP1), the normal mixture ($\mathrm{NM_K}$ or $\mathrm{NM_{Li}}$, with ^{40}K or ^{6}Li in excess, respectively), and the normal polarized (single-component) states ($\mathrm{NP_K}$ or $\mathrm{NP_{Li}}$). The phases are shown versus the population imbalance p and the normalized trap radius $\widetilde{r}$.

as one moves out from the trap center, the chemical potential monotonically decreases, while the superfluid order parameter is apparently not a monotonic function in this case. The superfluid only occurs in an intermediate shell. We will give some explanations for this unusual phenomenon later. Continuing with the phase diagram, if we increase the population of the heavy fermions, the central $\mathrm{NM_K}$ region grows, while the SF, $\mathrm{NM_{Li}}$, and the $\mathrm{NP_{Li}}$ phase regions shrink and finally all disappear at a critical population imbalance. After that, the trap edge is occupied by a single component normal gas of heavy fermions (denoted as $\mathrm{NP_k}$). If we increase the population of light fermions, the reverse happens. The central $\mathrm{NM_K}$ region shrinks and finally disappear at a critical population imbalance, and the superfluid shell evolves into a superfluid core.

On resonance (Fig. 1(b) with $(k_Fa_s)^{-1} = 0$), the superfluid phase region gets significantly larger. The normal mixture region $\mathrm{NM_{Li}}$ at the intermediate shell completely disappears, which is quite different from the equal mass case where there is always such a mixed shell [8]. Moving on to the BEC side of resonance with $(k_Fa_s)^{-1} = 0.2$ (Fig. 1(c)), the type-I breached pair phase (BP1) appears at an intermediate shell between the

SF and $\mathrm{NP_{Li}}$ phases, but only when the light fermions are in excess. Compared with the equal mass case [8], the critical $k_F a_s$ for the appearance of the BP1 state is significantly shifted towards the resonance point. Another notable feature at this $(k_F a_s)^{-1}$ is that when the heavy fermions are in excess, the superfluid shell is not surrounded a normal gas anymore. All the normal components are pushed to the central core. Further on to the BEC side with $(k_F a_s)^{-1} = 0.5$ (Fig. 1(d)), the normal mixture at the trap center finally disappears at all population imbalance, and we resume the picture of a superfluid core surrounded by a shell of a normal gas. The BP1 phase region at the intermediate shell grows as one expects, but again it only shows up when the majority is in the light fermions.

A remarkable feature from the above phase diagrams is that the superfluid forms a shell structure in space, which separates different types of normal states at the trap center and the edge. This feature is qualitatively different from the equal mass case. Now we would like to understand in more detail how this feature shows up. We know that the phase is determined by the global minimum of the thermo-potential Ω as a function of the gap Δ, under certain values of the chemical potentials $\mu_{\mathbf{r}}$ and h at the trap position $\mathbf{r}$. As one moves out from the trap center, $\mu_{\mathbf{r}}$ monotonically decreases as $\mu_{\mathbf{r}} = \mu - \widetilde{\mathbf{r}}^2$ (in the unit of E_F) while h remains the same. In Fig. 2(a), we show Ω as a function of Δ at several different values of the normalized radius $\widetilde{r}$ (thus with different $\mu_{\mathbf{r}}$). The values of h and the central μ are taken to be the typical ones for which there is a superfluid shell structure in the phase diagram. The potential Ω typically has a double-well structure. At the trap center (the lowest curve with $\widetilde{r} = 0$), the trivial well with $\Delta = 0$ is deeper which corresponds to a normal state. As one moves out, both wells are lifted, but with different speeds. At a lower critical value of $\widetilde{r}$ (which is 0.38 for the configuration in Fig. 2(a)), the two wells become equally deep. Above this value, the global minimum jumps to the nontrivial well with $\Delta \neq 0$, which signals a first-order phase transition to the superfluid state. As one moves further out, the nontrivial well approaches the trivial well; and at an upper critical value of $\widetilde{r}$ (which is 0.81 in Fig. 2(a)), the two wells merge, which signals a second-order phase transition from the superfluid to the normal state. Hence the potential Ω varies non-monotonically with $\mu_{\mathbf{r}}$, which leads to the superfluid shell state only at the intermediate region.

The above picture is established from the calculation of Ω. We can also give an intuitive explanation for the superfluid shell state. Note that except for the deep BEC side with a very strong coupling, it is always more favorable for the fermions to pair up when the mismatch of the Fermi surfaces of the two components becomes smaller. As one decreases the chemical potential $\mu_{\mathbf{r}}$ by moving out from the trap center, for non-interacting fermions

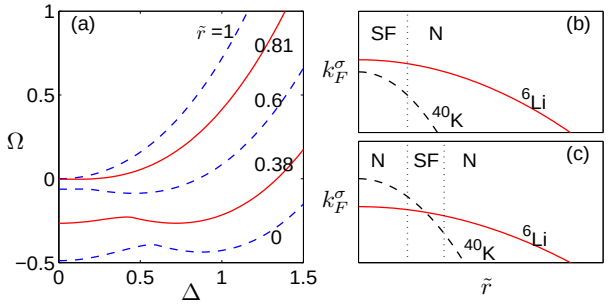

FIG. 2: (color online) (a) The thermodynamical potential Ω shown as a function of the order parameter Δ (both in the unit of E_F) at different trap positions (different chemical potentials) characterized by the normalized radius $\widetilde{r}$. The other parameters are $p = 0.2$, $T = 0$, and $(k_F a_s)^{-1} = 0$. The two solid curves bound a region corresponding to the SF phase, where the global minimum of Ω is at a nonzero Δ. (b) and (c) Schematic illustration of the radius of the Fermi surfaces k_F^σ for the two components as a function of the normalized trap radius $\widetilde{r}$. In (b), one can only have a superfluid core at the trap center, while in (c), one in general has a superfluid shell in the intermediate region.

the radius of the Fermi surface in the momentum space $k_F^\sigma(\widetilde{r})$ decreases as $k_F^\sigma(\widetilde{r}) = \sqrt{2m_\sigma(\mu_\sigma - \widetilde{\mathbf{r}}^2)}$ (in the standard unit) for the component σ. So, $k_F^\sigma(\widetilde{r})$ for the heavy fermions decreases faster with increasing $\widetilde{r}$. This qualitative statement should be true also for interacting fermions as interaction will not change the rough trend. Then, we can imagine two situations as depicted in Figs. 2(b) and 2(c). If at the trap center, the Fermi surface of the heavy fermions (^{40}K) has a smaller radius $k_F^\sigma(\widetilde{r} = 0)$ (Fig. 2(b)), the mismatch of the two Fermi surfaces only grows as one increases $\widetilde{r}$. Therefore the pairing superfluid, if any, can only form a core at the center. On the other hand, if the Fermi surface of the heavy fermions has a larger radius $k_F^\sigma(\widetilde{r} = 0)$ (which is the case when ^{40}K are in excess), the mismatch of the Fermi surfaces is minimized at an intermediate region (see Fig. 2(c)), so the superfluid only forms near that region and thus takes the shape of a spherical shell. This explains an important qualitative feature of the phase diagram in Fig. 1. As one further moves to the BEC side, the Fermi surface mismatch (and thus the above mechanism) becomes less important, and finally becomes independent as to which component is in excess. The superfluid then always forms a core at the trap center where there is a larger atomic density (Fig. 1(d)).

To detect the phase diagram of Fig. 1 in general and the superfluid shell state in particular, one can measure the atomic density profiles in the trap. The real-space density profiles for the polarized fermi gas have been measured in several experiments [1, 2, 3, 4]; in particular, the most recent one has shown how to reconstruct the full density profile from the column integrated signal [4]. We calculate the density profiles for several character-

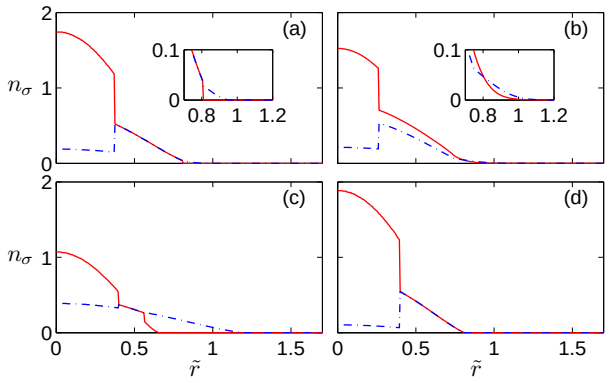

FIG. 3: (color online) The atomic number densities n_σ (in the unit of $n_F \equiv k_F^3/(3\pi^2)$) shown versus the normalized trap radius $\widetilde{r}$. The solid (dashed) curves are for the ^{40}K (^{6}Li) atoms, respectively. The inserts of (a) and (b) show the amplified tails of the density profiles. The other parameters are: (a)$T = 0$, resonance, and $p = 0.2$, (b) $T = 0.1T_F$, resonance, and $p = 0.2$, (c) $T = 0$, $(k_F a_s)^{-1} = -1$ (BCS side), $p = -0.4$, (d) $T = 0$, $(k_F a_s)^{-1} = 0.2$ (BEC side), $p = 0.3$.

istic configurations of phase separation, and the results are shown in Fig. 3. Figure 3(a) is for the resonance case with a small population imbalance $p = 0.2$ and at zero temperature. The superfluid shell (where the densities for the two components are equal) is clearly visible, which separates two normal regions. From the inside normal state to the superfluid, the heavy (light) fermion densities jump down (up), respectively. This jump is consistent with the first-order phase transition picture established from the thermodynamical potential Ω shown in Fig. 2(a). From the superfluid shell to the outside normal regions, the atomic densities drop continuously (consistent with the second-order phase transition picture in Fig. 2(a)). There is a small region of the $\mathrm{NM_{Li}}$ state, and outside is a tail for the $\mathrm{NP_{Li}}$ region. In Fig. 3(b), we show the finite temperature density profiles ($T = 0.1T_F$) with otherwise the same parameters as in Fig. 3(a). The profiles get a bit more smooth (as one expects), but the jump from the inside normal to the superfluid shell is still clearly visible. Note that as pointed out in Ref. [8], the densities are not equal any more for the BCS superfluid state at finite T since quasiparticle excitations carry population imbalance. Fig. 3(c) shows the density profiles on the BCS side. There are jumps in the density profiles from the superfluid shell to both the inside and the outside regions of normal states. Fig. 3(d) shows the profiles on the BEC side, still with a superfluid shell, but there is no normal region outside the shell any more (no tails with unequal densities). On the BEC side, there is also a region of the BP1 state at appropriate population imbalance. The BP1 state is hard to be directly seen from the real-space density profile, but can be unambiguously signaled with the detection of the momentum-space profile of the minority component [15].

In summary, we have mapped out the phase diagram of a strongly interacting fermion gas in a trap with both mass and population imbalance for the two spin components. As a remarkable feature, the superfluid forms a spherical shell in the case of mass mismatch. We attribute this phenomenon to a combined effect of the mass imbalance and the trapping potential. We also show that the superfluid shell should be clearly visible in experiments through explicit calculations of the atomic density profiles. The superfluid shell is not simply connected in space, so it should have nontrivial vortex properties under rotation of the trap, which is an interesting subject for future theoretical and experimental investigations.

This work was supported by the NSF awards (0431476), the ARDA under ARO contracts, and the A. P. Sloan Fellowship.

[1] M.W. Zwierlein, A. Schirotzek, C.H. Schunck, and W. Ketterle, Science 311, 492 (2006).
[2] G.B. Partridge, W. Li, R.I. Kamar, Y. Liao, and R.G. Hulet, Science 311, 503 (2006).
[3] M.W. Zwierlein, C.H. Schunck, A. Schirotzek, and W. Ketterle, Nature 442, 52 (2006).
[4] Y. Shin *et al.*, cond-mat/0606432.
[5] M. M. Forbes *et al.*, Phys.Rev.Lett. 94, 017001 (2005).
[6] P. F. Bedaque, H. Caldas, and G. Rupak, Phys. Rev. Lett. 91, 247002 (2003).
[7] D.E. Sheehy and L. Radzihovsky, Phys. Rev. Lett. 96, 060401 (2006); C.-H. Pao, S.-T. Wu, and S.-K. Yip, Phys. Rev. B 73, 132506 (2006).
[8] W. Yi and L.-M. Duan, Phys. Rev. A 73, 031604(R) (2006); W. Yi and L.-M. Duan, Phys. Rev. A 74, 013510 (2006).
[9] T.N. De Silva, E.J. Mueller, Phys. Rev. A 73, 051602(R) (2006); M. Haque, H.T.C. Stoof, cond-mat/0601321.
[10] P. Pieri, G.C. Strinati, Phys. Rev. Lett. 96, 150404 (2006); J. Kinnunen, L.M. Jensen, P. Torma, Phys. Rev. Lett. 96, 110403 (2006); F. Chevy, Phys. Rev. Lett. 96, 130401 (2006); T.-L. Ho and H. Zhai, cond-mat/0602568.
[11] C.-C. Chien, Q. Chen, Y. He, K. Levin, cond-mat/0605684.
[12] C. A. Stan et al., Phys. Rev. Lett. 93, 143001 (2004); S. Inouye et al., Phys. Rev. Lett 93, 183201 (2004).
[13] M. Iskin and and C. A. R. Sá de Melo, cond-mat/0604184; cond-mat/0606624.
[14] S.-T. Wu, C.-H. Pao, S.-K. Yip, cond-mat/0604572.
[15] W. Yi and L.-M. Duan, cond-mat/0605440.
[16] In this formalism, we neglect the FFLO state with condensation at non-zero pair momenta. The FFLO state can be stabilized only within a narrow parameter region on the BCS side [7]. The calculation in [7] is done for a homogeneous gas under a narrow Feshbach resonance, but we did similar calculation on the FFLO state under a wide Feshbach resonance and in a potential trap (W. Yi, G.-D. Lin, L.-M. Duan, unpublished), and find qualitatively the same conclusion.